INVESTIGATIONS OF THE FREQUENCY AND ELECTRIC FIELD STRENGTH DEPENDENCE OF FIELD GRADING MATERIALS FOR MEDIUM VOLTAGE CABLE ACCESSORY

Jun Ting Loh*, Mario Dreßler, Stefan Kornhuber

University of Applied Sciences Zittau/Görlitz, Theodor-Körner-Allee 16, 02763 Zittau

Irina Ovsyanko, Kai-Uwe Bentkowski

BBC Cellpack GmbH Carl-Zeiss-Straße 20, 79761 Waldshut-Tiengen

This contribution documents the preliminary investigations on two different elastomeric field grading materials designed for medium voltage cable accessory. The dielectric properties of the materials are determined under variable frequencies and electric field strengths, measured using three different setups. The experimental results provide fundamental insights into the material behaviour under high frequency stress and can be implemented in the future to model field grading behaviour under the influence of harmonics.

1. Motivation

Electric field grading refers to the technique of reducing local field enhancement on interfaces in insulation systems, which prevents the dielectric strength of the insulation materials from being exceeded and is thus crucial in ensuring the reliability of the insulation system. In the case of a medium voltage power cable, the "triple point" between the conductive layer of the cable, cable insulation and cable accessory would face the highest electric field. In this case, a field grading material is mounted onto this interface to ensure appropriate field distribution. Depending on the type of the voltage stress, different field grading techniques are applied. Field grading can either be achieved by increasing the electrode radius (geometric field grading), or by implementing materials of different conductivities (resistive field grading) or permittivities (refractive field grading) [1], [2].

Besides that, nonlinear field grading materials are also implemented in commercially available products, mainly by implementing microvaristors such as zinc oxides (ZnO), or semiconductors such as silicone carbides (SiC) or carbon black as functional fillers [1], [3]–[5]. Such materials first exhibit a linear current-voltage relationship. Above a certain level of the voltage and thus exceeding the material's

switching field, the current will experience a sharp increase, thus leading to a nonlinear increase of the power loss.

While field grading for standardized voltage stress such as DC, AC and transient voltages are well known, their response towards nonstandardized voltage stresses, such as when harmonics are present, requires more research. Harmonics with frequencies higher than the operational frequency of 50 / 60 Hz are, for example, induced by the implementation of power electronics in electrical grids. Such high frequencies causes distortion in the sinusoidal voltage stress, resulting in additional electrical stress in the insulation systems, leading to a shorter operational lifetime of the electrical component [6]-[8]. For example, studies from [8] have shown that resistive field grading materials are prone to local temperature increase due to the high frequencies, leading ultimately to the failure of cable terminations. Studies have also proven that altered partial discharge behaviour such as the PD intensity due to harmonics cannot be ruled out [9].

To properly design the field grading system as well as for the construction of the cable accessory, it is important to ensure that the field grading materials withstand such electrical stress. This contribution presents the preliminary investigations on different field grading

materials; dielectric properties such as the permittivity ε_r , dielectric loss tangent tan δ and the DC-conductivity σ_{DC} are determined under variable frequencies and electric field strengths.

2. Experimental Approach

2.1. Test Samples

Two different elastomers with a thickness d of 1 mm are tested. All elastomers are designed as field grading materials in medium voltage cable accessories.

The samples are conditioned in an oven at 90 °C for 96 h before the start of every experiment to remove moisture in the sample. All experiments are conducted with a guard ring electrode arrangement with an effective area $A_{\rm m}$ of 20 cm² according to [10] at room temperature (23 °C).

2.2. Test Setup and Procedure

2.2.1. Electrical Conductivity at DC-Voltages

A relevant material property to evaluate field grading is the conductivity σ_{DC} , which is determined under DC-voltage. The conductivity is measured for 24 h using an electrometer (Sefelec Megaohmmeter) up to an electric field strength of 1 kV/mm.

$$\sigma_{\rm DC} = \frac{I_{\rm DC} d}{U_{\rm DC} A_{\rm M}} \tag{1}$$

2.2.2. Capacitance and Dielectric Loss Tangent Measurement at 50 Hz

To obtain the electric field dependence, investigations are conducted using the capacitance and $\tan \delta$ measuring system Tando 700 with an external voltage source up to 2 kV. The drawback with this equipment is the fact that only measurements at 50 Hz can be conducted.

2.2.3. Frequency-Domain-Spectroscopy

Meanwhile, the frequency response of the samples is measured by conducting a frequency sweep from 0.1 mHz to 5 kHz (FDS-Analysis). The measurements are conducted using the test system Spectano 100, which supplies voltages up to 200 V_{peak} .

2.2.4. Dielectric Measurements at High Frequency AC-Voltages

In order to determine the frequency response of the dielectric properties at higher voltages, the voltage and current measurements are conducted at variable frequencies. By calculating the active power P, the apparent power S and the reactive power Q based on the measured voltage u(t) and current i(t), the dielectric loss tangent tan δ as well as the permittivity ε_r can then be deduced (2)-(3). The construction of the test setup and methods are described in detail in [11]. With this test setup, measurements up to U=1 kV and f=1950 Hz are possible.

$$\tan \delta = \frac{P}{O} \tag{2}$$

$$\varepsilon_r = \frac{Qd}{\omega \varepsilon_0 A_{\rm M} U_{\rm rms}^2} \tag{3}$$

3. Results and Discussion

3.1. Electrical Conductivity at DC-Voltages

Figure 1 compares the electrical conductivity σ_{DC} of both FGM as a function of the electric field strength E.

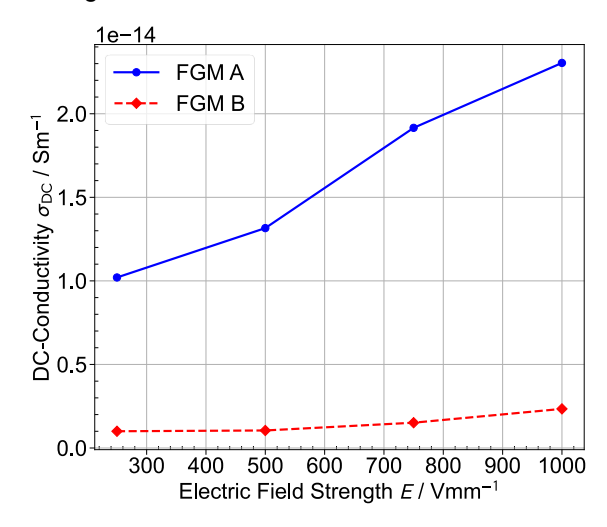


Figure 1: Electric Field Dependence of the DC-Conductivity σ_{DC}. One sample each.

Generally, the conductivity of FGM A lies at 10^{-14} S/m and is about one order of magnitude higher than that of FGM B, which is around 10^{-15} S/m. For both FGM, the conductivity σ_{DC} increases with increasing electrical field strength.

Due to time constraints, only one sample per material is measured for each electric field strength. While these results are not statistically significant, they do provide a rough sense of orientation regarding the range in which the conductivity lies respectively. For statistical significance, a higher number of test samples is required.

3.2. Permittivity and Dielectric Loss Tangent

3.2.1. Electric Field Dependence at 50 Hz

Figure 2 depicts the electric field dependence of both the permittivity ε_r and dielectric loss tangent tan δ , measured at the frequency 50 Hz.

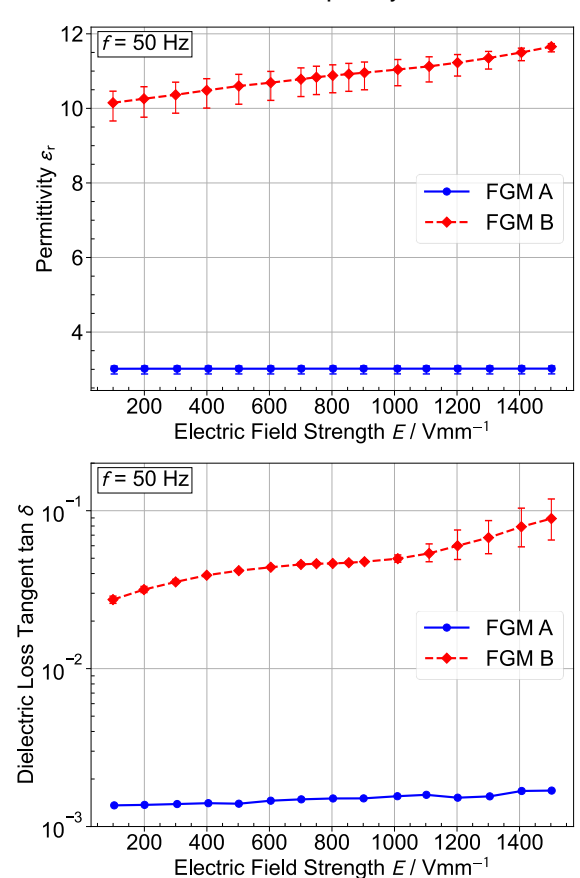


Figure 2: The electric field dependence of (a) the permittivity ε_r and (b) the dielectric loss tangent tan δ, measured at the frequency of 50 Hz. Three samples each.

Within the tested range, the influence of the electric field strength on the permittivity ε_r of FGM A is deemed insignificant (**Figure 2a**). In comparison to that, the permittivity ε_r of FGM B shows a linear increase from 10 to 12 as the electric field strength increases from 100 V/mm to 1500 V/mm.

Figure 2b shows that the influence of the electric field strength up to 1,5 kV/mm is negligible in FGM A. Meanwhile, the dielectric loss tangent tan δ of FGM B exhibits a nonlinear field strength dependence. Tan δ first increases slightly from 0.03 to 0.05 with increasing electric field strength up to 1000 V/mm, from 1000 V/mm onwards a drastic increase can be seen, where tan δ = 0.08 ± 0.02 at the electric field strength of 1500 V/mm is double the value at 1000 V/mm. The linear behaviour of FGM B's permittivity observed in **Figure 2a** suggests that the

nonlinear dielectric loss tangent from FGM B stems from a nonlinear conductivity, which is activated once the electric field strength of 1000 V/mm is exceeded. However, further measurements of the conductivity at higher levels of voltages are required to prove this theory.

3.2.2. Frequency Domain Spectroscopy

Figure 3 compares the frequency response of the permittivity ε_r and the dielectric loss tangent tan δ of both materials, measured at E = 200 V/mm.

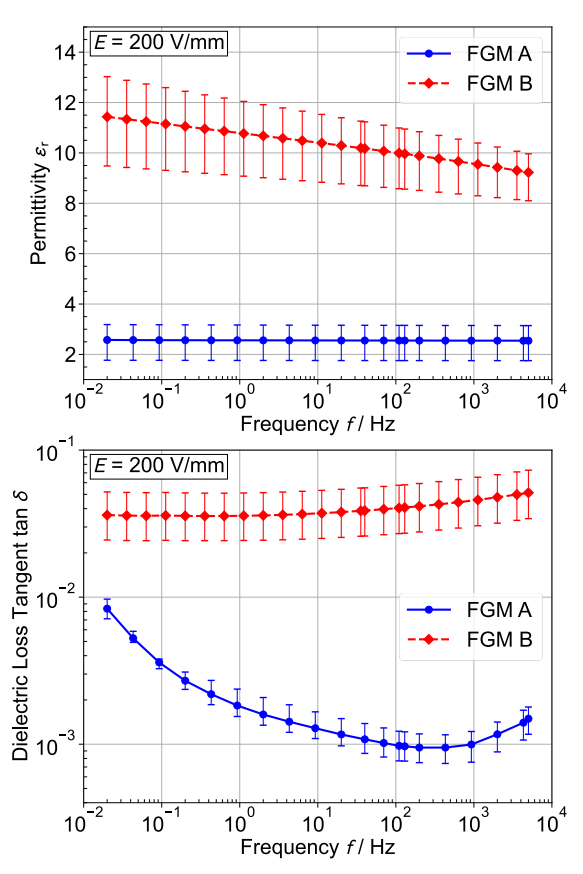


Figure 3: The frequency response of (a) permittivity ε_r and (b) the dielectric loss tangent tan δ, measured at the electric field strength of 200 V/mm. Three samples each.

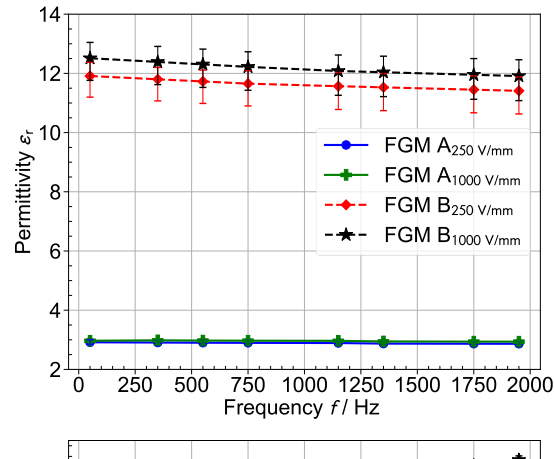
Figure 3a shows that FGM A has a permittivity of $\varepsilon_r = 2.6 \pm 0.4$ and that the frequency dependence is insignificant, leading to the assumption that FGM A has a low filler content. As opposed to that, FGM B has a higher permittivity with $\varepsilon_r = 10 \pm 1$ at 50 Hz, which generally decreases with increasing frequency. This decrease is due to the delayed motion of the dipoles according to the field direction at higher frequencies, causing a weaker polarizability [12]. The dominant process here is interfacial polarization between the functional fillers and insulating matrix in FGM B. This in return results in higher polarization losses, which is reflected in

the increasing dielectric loss tangent tan δ of FGM B as frequency increases (**Figure 3b**).

In general, the dielectric loss tangent tan δ of FGM B is higher than that of FGM A (**Figure 3b**). At the lowest frequency of 10 mHz, FGM B has a dielectric loss tangent of tan δ = 0.035 ± 0.015, which increases slightly up to 0.05 ± 0.015 with increasing frequency up to 5 kHz. Meanwhile, the characteristics of FGM A resembles a distinctive bathtub curve, with the turning point of tan δ = 0.001 ± 0.0004 at 100 Hz. With decreasing frequencies from 100 Hz to 10 mHz, tan δ increases by a factor of ten, which can be attributed to increased conduction loss. Beyond 100 Hz, tan δ continues to increase again but without significance.

3.2.3. Frequency Response at High Voltages

Figure 4 compares the frequency response of both FGM at higher voltages and at frequencies between 50 Hz and 2000 Hz, determined using the current-voltage measurements up to E = 1 kV/mm.



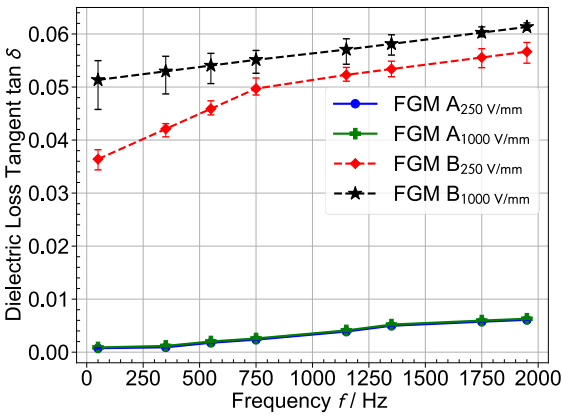


Figure 4: Frequency response of FGM A and FGM B at E = 250 V/mm and E = 1 kV/mm

The results show that up to 1 kV/mm, the influence of the electric field strength on the permittivity and the dielectric loss tangent of FGM A are negligible. Besides that, between

frequencies 50 Hz and 2000 Hz, the permittivity stays constant at $\varepsilon_r = 3$. The increase of the dielectric loss tangent tan δ is comparable to the values determined via FDS-analysis.

For FGM B, both permittivity ε_r and dielectric loss tangent tan δ are dependent on the frequency and electric field. Between 50 Hz and 2000 Hz, the permittivity ε_r sinks slightly with increasing frequency, but increases with increasing electric field strength. Interestingly, at 500 V/mm, two different gradients are observed in the dielectric loss tangent tan δ . At 1000 V/mm, this nonlinearity vanishes and the dielectric loss tangent increases linearly with increasing frequency.

3.3. Nonlinear Current Response

Nonlinear behaviour of a material refers to a nonlinear current response to an applied electric field $E = E\cos(\omega t)$. For example, in **Figure 5**, the nonlinearity of FGM B is observed by the distortion in the measured current signal (I_{meas}) under a sinusoidal voltage stress (U_{meas}).

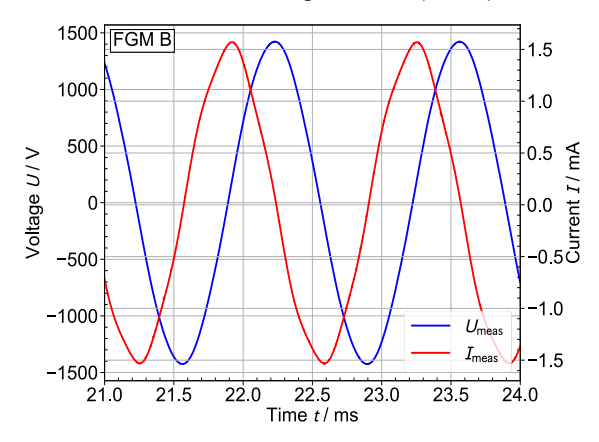


Figure 5: Distorted current signal due to material's nonlinearity in relation to a sinusoidal voltage

The presence of nonlinearities suggests that additional harmonic terms are existent, resulting in the distorted current form [13]. Given that only the total current can be experimentally measured, mathematical separation of the total current into its resistive l_{res} and capacitive component l_{cap} provides insight into whether the electrical conductivity (*nonlinear resistive*) or the permittivity (*nonlinear refractive*) is field-dependent [13]–[15].

For appropriate design and construction, an important parameter for nonlinear field grading is the switching field E_s of the material, which specifies the threshold electric field required to induce the sharp change in the conductivity or permittivity [1]. To determine the switching field E_s of the FGM A, additional measurements

of the voltage and current characteristics are conducted at higher voltages up to 4 kV at 50 Hz. The total current $I_{\rm meas}$ is then separated into its resistive $I_{\rm res}$ and capacitive component $I_{\rm cap}$ respectively using equation (4), with φ defined as the phase difference between the voltage and current.

$$I = I_{res} + I_{cap} = I\cos(\varphi) + I\sin(\varphi)$$
 (4)

Figure 6 illustrates the respective current components in relation to the voltage.

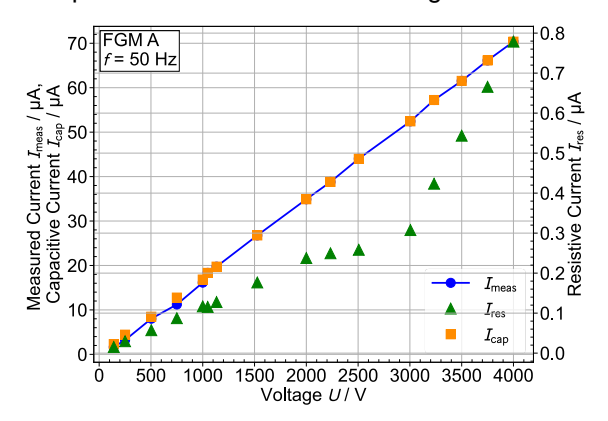


Figure 6: The measured current I_{meas} and its respective resistive I_{res} and capacitive current I_{cap}, plotted against the voltage U

With the capacitive current I_{cap} being the dominant component of the measured current, the resistive current I_{res} is two orders of magnitude lower than the capacitive current I_{cap} . While the capacitive current is proportional to the voltage, the resistive current experiences a sharp increase above 3000 V, indicating a distinct increase in the conductivity of FGM A. Not shown here is that throughout the measurements up until 4 kV, the permittivity remains constant at $\varepsilon_r = 3$, further confirming that it is independent of the electric field.

Figure 7 compares the *U-I_{res}*-relationship between FGM A and FGM B. In comparison to FGM A, the resistive current *I_{res}* of FGM B is not only around one order of magnitude higher, the slope of the increase in *I_{res}* with increasing voltage is also steeper. The turning point of the curve, which indicates nonlinearity, is recorded at 1000 V. For FGM A, the resistive current increases at a slower rate; the turning point of the curve only appears at 3000 V.

With knowledge of the dielectric properties at higher frequencies, FEM-models of the FGM in practical applications, such as end terminations,

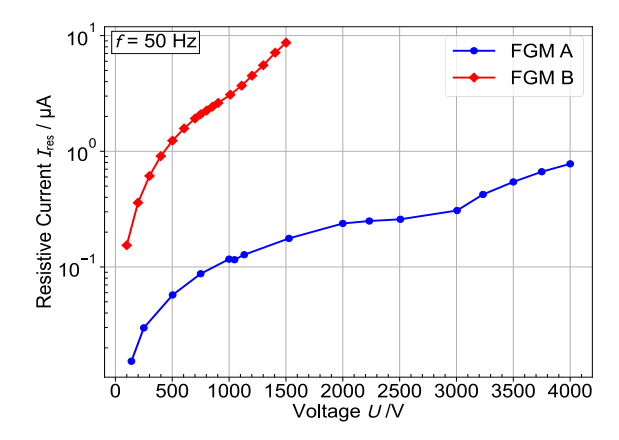


Figure 7: Comparison of the U-I-characteristics in terms of the resistive current I_{res} as a function of voltage

can be simulated to analyse their field grading behaviour at operational stresses with high frequencies as well as under the influence of harmonics (superimposed AC+AC). Considering that the resistive current plays an important part here, evaluation of the joule losses would also be of benefit.

4. Summary and Conclusion

This contribution presents the dielectric properties of two different field grading materials in terms of their conductivity at DC as well as the permittivity and dielectric loss tangent at AC, under the influence of high frequencies. Two different behaviours regarding the frequency dependence are recorded. The dielectric behaviour of FGM A remain mainly unaffected by frequencies up to 2 kHz, whereas FGM B shows a frequency dependence. Nevertheless, the change in permittivity and dielectric loss tangent with increasing frequencies insignificant and still remains within deviations of material production. Judging from these results, no negative conclusions regarding reliability of medium voltage cable accessories can be drawn. Both FGM exhibit nonlinear field dependence, albeit at different field strengths. The difference between these two materials is largely attributed to the different functional fillers applied for field grading. Based on the experimental results, FEM simulations to assess the impact of high frequencies and estimate the influence of harmonics on the electric field distribution in medium voltage cable accessories are in progress.

Acknowledgements

The authors would like to thank BBC Cellpack Electrical Products for providing the specimens.

Literatur

- [1] CIGRE WG D1.56, Field grading in electrical insulation systems, 794 vols. Paris: CIGRE, 2020.
- [2] V. Hinrichsen and A. Küchler, 'Grundlagen der Feldsteuerung', in Feldsteuernde Isoliersysteme: Werkstoffe, Design, Prüfung und Simulation, Darmstadt: VDE Verlag GmbH, 2011.
- [3] T. Christen, L. Donzel, and F. Greuter, 'Nonlinear resistive electric field grading part 1: Theory and simulation', *IEEE Electrical Insulation Magazine*, vol. 26, no. 6, pp. 47–59, Nov. 2010.
- [4] R. Hussain, 'Elektrische Charakterisierung von Flüssigsilikonelastomer mit nanoskaligem Carbon Black für den Einsatz in HGÜ-Kabelgarnituren', Dissertation, Technische Universität Darmstadt, Darmstadt, 2021
- [5] R. Bärsch and J. Kindesberger, 'Nichtlineare dielektrische Funktionseigenschaften von Dielektrika', in ETG-Fachbericht 110, Stuttgart: VDE Verlag GmbH, Mar. 2008.
- [6] L. Paulsson et al., 'High-frequency impacts in a converter-based back-to-back tie; The Eagle Pass installation', IEEE Transactions on Power Delivery, vol. 18, no. 4, 2003.
- [7] M. Birle, 'Beanspruchung von Polymeren durch höherfrequente Anteile einer Mischspannung', Dissertation, Shaker, Aachen, 2015.
- [8] M. Li, F. Sahlen, S. Halen, G. Brosig, and L. Palmqvist, 'Impacts of high-frequency voltage on cable-terminations with resistive stress grading', in *Proceedings of* the 2004 IEEE International Conference on Solid Dielectrics, 2004.
- [9] M. Florkowski, B. Florkowska, J. Furgał, and P. Zydron, 'Impact of high voltage harmonics on interpretation of partial discharge patterns', *IEEE Transactions on Dielectrics and Electrical Insulation*, vol. 20, no. 6, pp. 2009–2016, Dec. 2013.
- [10] DIN EN IEC 62631-2-1: Dielektrische und resistive Eigenschaften fester Elektroisolierstoffe – Teil 2-1: Dielektrizitätszahl und der Verlustfaktor
- [11] T. Linde, J. T. Loh, S. Kornhuber, K. Backhaus, S. Schlegel, and S. Großmann, 'Implications of Nonlinear Material

- Parameters on the Dielectric Loss under Harmonic Distorted Voltages', *Energies*, Jan. 2021.
- [12] K. C. Kao, Dielectric Phenomena in Solids - With Emphasis on Physical Concepts of Electronic Processes. Elsevier Academic Press, 2004.
- [13] T. Christen, R. Kochetov, and L. Almquist, 'High-voltage low-frequency dielectricspectroscopy used for characterization of nonlinear insulation materials', in 2016 IEEE International Conference on Dielectrics (ICD), Jul. 2016.
- [14] J. T. Loh and S. Kornhuber, 'Characterization of Silicone Elastomers for Refractive Field Grading under Sinusoidal Voltages', Proceedings of the Nordic Insulation Symposium, Jul. 2022.
- [15] S. Blatt and V. Hinrichsen, 'Mathematical model for numerical simulation of current density in microvaristor filled insulation materials', IEEE Transactions on Dielectrics and Electrical Insulation, Apr. 2015